Multidimensional scaling analysis of fractional systems

J. Tenreiro Machado

A B S T R A C T

This paper investigates the use of multidimensional scaling in the evaluation of fractional system. Several algorithms are analysed based on the time response of the closed loop system under the action of a reference step input signal. Two alternative performance indices, based on the time and frequency domains, are tested. The numerical experiments demonstrate the feasibility of the proposed visualization method.

Keywords:
Fractional calculus
Multidimensional scaling
Control

1. Introduction

Fractional Calculus (FC) represents the generalization of the classical integer-order differential calculus. FC was triggered by a question posed in a correspondence between Leibniz and l'Hôpital [1–3]. Nevertheless, FC is currently considered as an important topic because during the past decades relevant studies emerged in many scientific areas [4–11] motivating an increasing interest in its application. Due to this fact researchers are paying considerable attention to fractional algorithms, but the proposed mathematical and computational tools are still far from leading to straightforward and simple results.

Bearing these ideas in mind, this paper studies the application of multidimensional scaling (MDS) visualizing technique for comparing fractional order systems, and is organized as follows. Section 2 introduces the MDS concepts. Section 3 develops numerical experiments with linear systems under the action of fractional control algorithms. Finally, Section 4 outlines the main conclusions.

2. Multidimensional scaling

MDS is a technique used for visualization information in the perspective of exploring similarities in data [12–19]. MDS assigns a point to each item in a multi-dimensional space and arranges them in order to reproduce the observed similarities. Often, instead of similarities are considered dissimilarities, or distances, between the objects. For two or three dimensions the resulting locations may be displayed in a 'map' that can be analysed.

An MDS algorithm starts by defining a measure of similarity (or, alternatively, of distance) and to construct a square matrix of item to item similarities (or, alternatively, of distances). In classical MDS the matrix is symmetric and its main diagonal is composed of '1' for similarities (or of '0' for dissimilarities). MDS is a procedure that tries to rearrange objects so as to arrive at a configuration that best approximates the observed similarities (or distances). For this purpose MDS uses a function minimization algorithm that evaluates different configurations with the goal of maximizing the goodness-of-fit. The most common measure that is used to evaluate how well a particular configuration reproduces the observed distance matrix is the raw stress measure defined by $S = \left[\sum d_{ij} - f\left(\delta_{ij}\right)\right]^2$ where d_{ij} stands for the reproduced distances, given the respective number of dimensions, and δ_{ij} represents the input data (i.e., the observed distances). The expression $f\left(\delta_{ij}\right)$ indicates a nonmetric, monotone transformation of the input data. Thus, the smaller the stress value S, the better is the fit between the reproduced and the observed distance matrices. We can plot S versus the number of dimensions for deciding the 'best' one.

Usually we get a monotonic decreasing plot and we chose the 'best' dimension as a compromise between stress reduction and dimension for the map representation. In practical terms, we chose a low dimension at the region where we have a significant 'elbow' in the stress plot.

We can also plot the reproduced distances, for a particular number of dimensions of the MDS map, against the observed input data (distances). This scatter plot, referred to as Shepard diagram, shows the distances between points versus the original dissimilarities. In the Shepard plot, a narrow scatter around a 45° indicates a good fit of the distances to the dissimilarities, while a large scatter indicates a lack of fit.

3. Analysis of fractional control algorithms

In this section, we apply classical MDS for visualizing the performance of several approximations of fractional control algorithms [20–22]. For obtaining the discrete time algorithms, that is, for converting expressions from continuous to discrete time, are often considered the Euler and Tustin expressions:

$$H_0^{\alpha}\left(z^{-1}\right)=\left[\frac{1}{T_s}\left(1-z^{-1}\right)\right]^{\alpha} \tag{1}$$

$$H_1^{\alpha}\left(z^{-1}\right)=\left[\frac{2}{T_s}\frac{1-z^{-1}}{1+z^{-1}}\right]^{\alpha} \tag{2}$$

where z and T_s represent the Z-transform variable and controller sampling period, respectively. The Euler expression is, in fact, a direct result of the Grünwald–Letnikov definition of fractional derivative with the infinitesimal time increment h replaced simply by the sampling period T. Weighting H_0 and H_1 by the factors p and $1-p$, leads to the arithmetic average:

$$H_{av}^{\alpha}\left(z^{-1}\right)=pH_0^{\alpha}\left(z^{-1}\right)+(1-p)\,H_1^{\alpha}\left(z^{-1}\right). \tag{3}$$

The so called Al-Alaoui operator corresponds to an interpolation of $H_0^{\alpha}\left(z^{-1}\right)$ and $H_1^{\alpha}\left(z^{-1}\right)$ with weighting factor $p=\frac{3}{4}$ [23–25].

In [26] were studied other averages based on the generalized mean, but in this paper those expressions are not considered for the sake of simplification.

In order to obtain rational expressions usually are adopted Taylor or Padé expansions of order r, in the neighbourhood of $z=0$, leading to series and fractions of the type:

$$T_r^{\alpha}\left(z^{-1}\right)=\sum_{i=0}^{r}a_i z^{-i},\quad a_i\in R \tag{4}$$

$$P_r^{\alpha}\left(z^{-1}\right)=\frac{\sum_{i=0}^{r}a_i z^{-i}}{\sum_{i=0}^{r}b_i z^{-i}},\quad a_i,\,b_i\in R. \tag{5}$$

Having these ideas in mind [27], we start the MDS method by establishing a first measure of comparison based on the closed-loop system response to an input step reference signal. Therefore, we define the normalized time correlation index:

$$c_{lr}=\frac{\left|\sum_{t=0}^{T_w}x_l(t)x_r(t)\right|}{\sqrt{\sum_{t=0}^{T_w}x_l^2(t)\sum_{t=0}^{T_w}x_r^2(t)}} \tag{6}$$

where t denotes time, $x_l(t)$ and $x_r(t)$ represent the l-th and r-th output signals, and T_w is the time window of the calculation. This expression uses the inner product of vectors and is often denoted as cosine correlation [28].

With this measure we can now implement a matrix $\mathbf{C}=[c_{lr}]$ of dimension 29×29 that feeds the MDS algorithm when construct the maps.

During the numerical calculations was adopted a sampling period of $T=0.1$ s and a time window of $T_w=100$ s.

Our test bed consists of twenty nine systems (see Table 1) with unit feedback subjected to a reference unit step input, and correspond to combinations of the transfer functions of the fractional control algorithm $G_c(s)$, $\alpha=0.5$, and the process $G_p(s)=\frac{1}{s^2}$. In the fractional control algorithms are considered the ideal case $G_c(s)=s^{0.5}$ (labelled ML as it adopts the Mittag-Leffler function denoted by $E_{\alpha}(),\alpha>0$) leading to the closed-loop response $y(t)=1-E_{0.5}\left(-t^{0.5}\right)$, the Taylor $T_r^{0.5}\left(z^{-1}\right)$ and Padé $P_r^{0.5}\left(z^{-1}\right)$ expansions (labelled as T and P) of order $r=\{1,\ldots,7\}$ (labelled from 1 up to 7), based on the Grünwald–Letnikov and Al-Alaoui formulae (labelled as G and A),

Table 1
System characteristics.

Label	$G_c(s)$	Approximation
ML	$G_c(s) = s^{0.5}$	No
TrG	$T_r^{0.5}\left(z^{-1}\right)$	Taylor, order r, Grünwald–Letnikov
PrG	$P_r^{0.5}\left(z^{-1}\right)$	Padé, order r, Grünwald–Letnikov
TrA	$T_r^{0.5}\left(z^{-1}\right)$	Taylor, order r, Al-Alaoui
PrA	$P_r^{0.5}\left(z^{-1}\right)$	Padé, order r, Al-Alaoui

Figs. 1 and 2 depict the corresponding MDS maps for two and three dimensions, and Figs. 3 and 4 show the corresponding Shepard diagrams. Finally, Fig. 5 represents the stress plot.

The three dimensional plot leads to a slightly better visualization than the two-dimensional counterpart. Therefore, the three-dimensional map is followed in the sequel. In general the Padé perform better than the Taylor and the Al-Alaoui seems slightly superior to the Grünwald–Letnikov. Nevertheless, the Al-Alaoui depicts some instability with the odd order approximations clearly better than the even orders. The second aspect to highlight is the pattern revealed in the plot. We have the low order approximations {T1G, T2A, P1A} far away from the rest of the cases that form a queue pointing towards the ML point. The queue is composed by the points {T4A, P1G, P3G, T1A, T2G, T6A, T4G, P2A, T5G, T3A, T6G, T7G, P2G, P3A, T5A, T7A}. Close to the ML point we get an arc composed by {P7G, P6G, P5G, P7A, P4G, P6A, P5A, P3G, P4A}. The 'best' points are {P5A} and {P6A} and, therefore, it seems that superior orders in the Padé have some kind of drawback. We can also compare partial clusters. For example, just to mention one case, the group {T6A, T4G, P2A} are close together (i.e., they are similar) in the perspective of the proposed methodology.

With MDS we have freedom to chose several distance measures that capture differently the system characteristics. Therefore, distinct performance indices lead to different MDS maps and the choice of the 'best' chart depends on the researcher habitability to interpret each one.

We now consider the Fourier transform of the system time responses for designing a second index:

$$\begin{aligned} c_{lr} &= \left[1 + \sum_{\omega=\Omega_{\min}}^{\Omega_{\max}} \left(\Delta\mathrm{Re}^2 + \Delta\mathrm{Im}^2\right)\right]^{-1} \\ \Delta\mathrm{Re} &= \mathrm{Re}\left\{X_l\left(j\omega\right)\right\} - \mathrm{Re}\left\{X_r\left(j\omega\right)\right\} \\ \Delta\mathrm{Im} &= \mathrm{Im}\left\{X_l\left(j\omega\right)\right\} - \mathrm{Im}\left\{X_r\left(j\omega\right)\right\} \end{aligned} \tag{7}$$

where ω denotes the angular frequency, $X_l\left(j\omega\right)$ and $X_r\left(j\omega\right)$ represent the Fourier transforms of the l-th and r-th signals, $\Omega_{\min}$ and $\Omega_{\max}$ are the bandwidth limits and $j = \sqrt{-1}$.

In the experiments was adopted $\Omega_{\min} = 0.1$ and $\Omega_{\max} = 10$ (rad/s) and a set of 200 sampling frequencies. We observe a distinct grouping from the one obtained with the time correlation measure, although the global conclusions are of the same type.

We have two groups, namely the {T4G, P2A, T6A} and {T3G, T1G, T2A, P1A, P1G, T4A, T2G, T1A}, very far away from the ML point, followed by a queue of {T5G, T3A, T6G, T7G, P2G, P3A, T5A, T7A, P4A, P3G} pointing towards ML. Finally, near the ML we observe the point {P5A}, which is the 'best', while the cluster {P4G, P6A, P7G, P6G, P5G, P7A} is slightly apart, probably due to numerical round-off errors.

Figs. 6 and 7 depict the MDS maps for two and three dimensions, Figs. 8 and 9 show the corresponding Shepard diagrams and Fig. 10 represents the stress plot.

It should be noted that we get distinct MDS maps in the two approaches, since measures (6) and (7) capture distinct dynamical characteristics. However, in both cases we get a representation that makes sense when we compare the position of the points representing the distinct systems.

The comparison of the MDS maps based in two alternative indices seems to point towards (6) since it is slightly simpler to calculate and, on the other hand, leads to superior Shepard and stress charts. However, the application with other expressions and systems may prove otherwise and researchers should test each case before making a definitive assessment.

In conclusion, we verify that MDS constitutes a mathematical tool capable of representing fractional systems without being limited to a particular class of expressions or of measuring indices. Therefore, the results motivate further studies using other distance measures and new classes of fractional algorithms.

4. Conclusions

In this paper was studied the application of MDS in the analysis of fractional approximating algorithms in control systems. The method relies on comparing different groups and patterns that emerge in the map representation. The study addressed the time response of systems subjected to a step reference input but its generalization to other tests and distance measures is straightforward. The results demonstrate the feasibility of the proposed method, revealing that it is simple for performing the numerical comparison and graphical visualization of different systems.

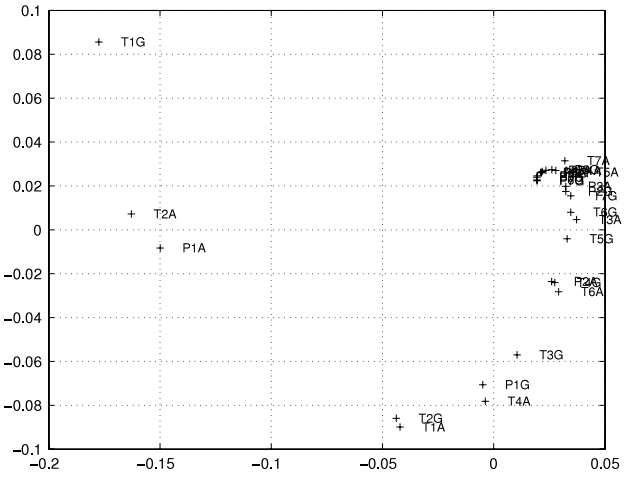

Fig. 1. Two dimensional MDS map based on the signal time correlation index (6).

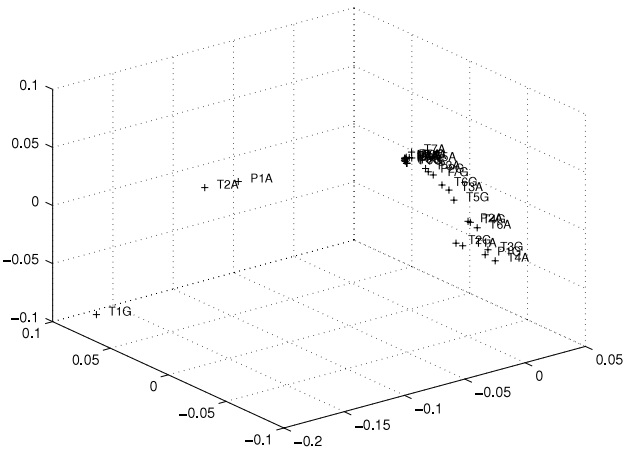

Fig. 2. Three dimensional MDS map based on the signal time correlation index (6).

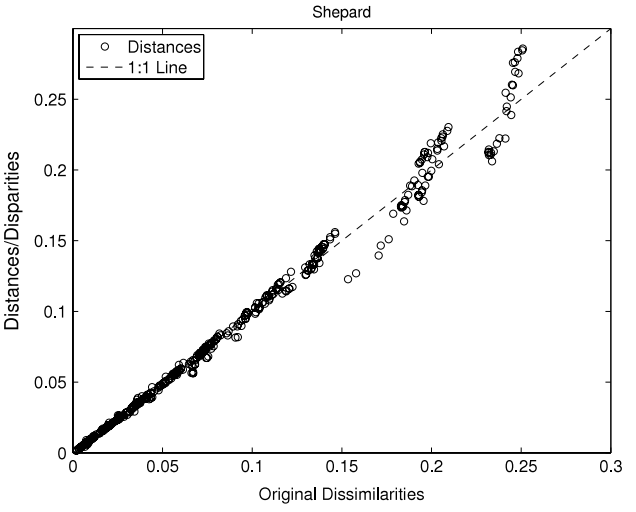

Fig. 3. Shepard diagram for the two dimensional MDS map based on signal time correlation index (6).

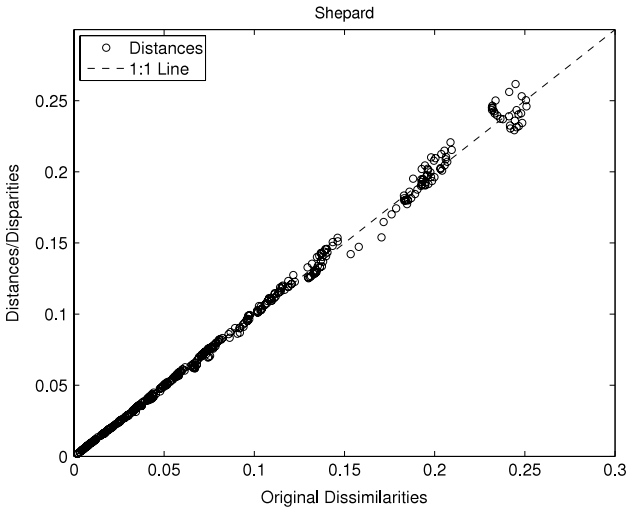

Fig. 4. Shepard diagram for the three dimensional MDS map based on signal time correlation index (6).

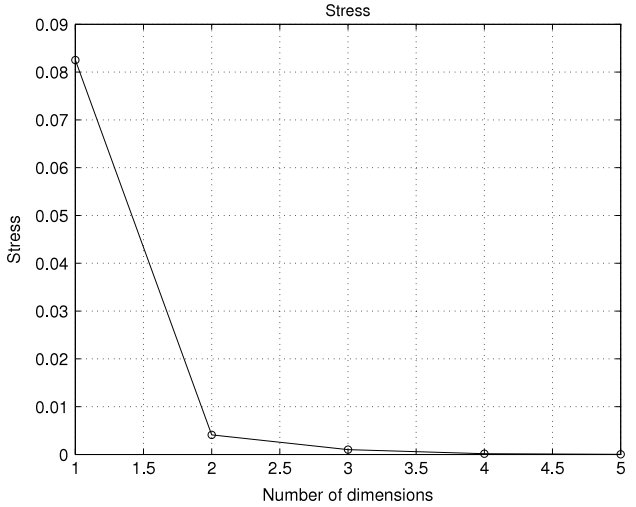

Fig. 5. Stress versus number of dimensions for the MDS maps based on signal time correlation (6).

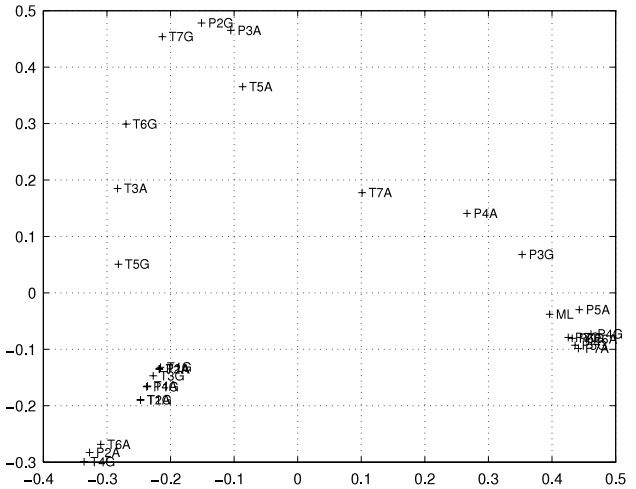

Fig. 6. Two dimensional MDS map based on the signal frequency response index (7).

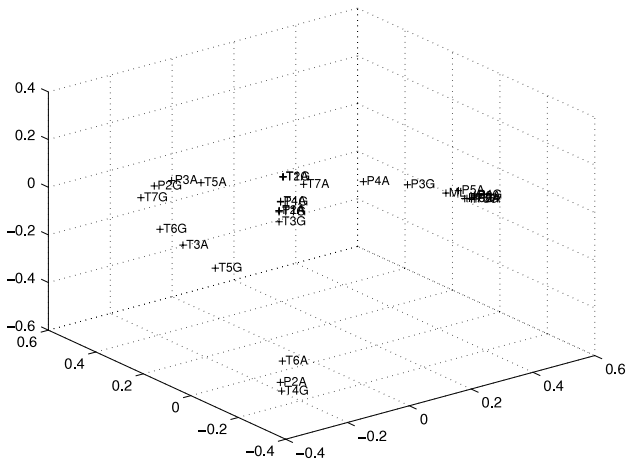

Fig. 7. Three dimensional MDS map based on the signal frequency response index (7).

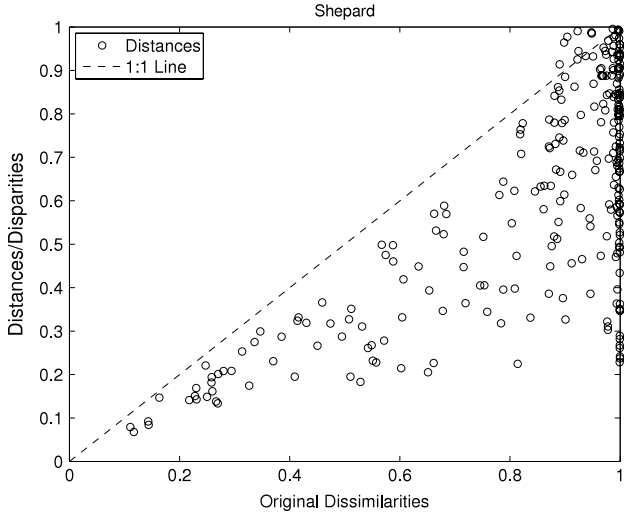

Fig. 8. Shepard diagram for the two dimensional MDS map based on frequency response index (7).

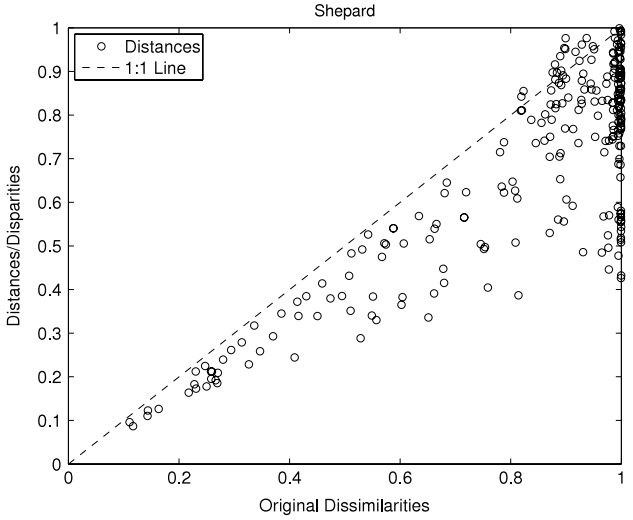

Fig. 9. Shepard diagram for the three dimensional MDS map based on frequency response index (7).

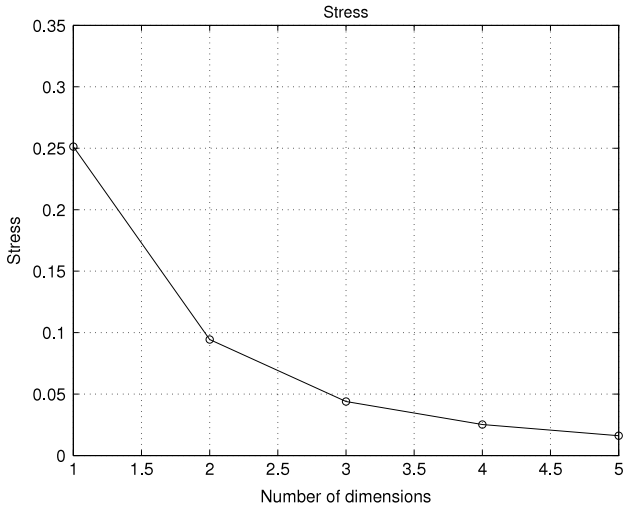

Fig. 10. Stress versus number of dimensions of the MDS maps based on frequency response index (7).

References

[1] K.B. Oldham, J. Spanier, The Fractional Calculus: Theory and Application of Differentiation and Integration to Arbitrary Order, Academic Press, New York, 1974.
[2] I. Podlubny, Fractional Differential Equations, Volume 198: An Introduction to Fractional Derivatives, Fractional Differential Equations, to Methods of their Solution, Mathematics in Science and Engineering, Academic Press, San Diego, 1998.
[3] H.M.S.A.A. Kilbas, J.J. Trujillo, Theory and Applications of Fractional Differential Equations, in: North-Holland Mathematics Studies, vol. 204, Elsevier, Amsterdam, 2006.
[4] F. Mainardi, Fractional relaxation–oscillation and fractional diffusion-wave phenomena, Chaos, Solitons & Fractals 7 (6) (1996) 1461–1477.
[5] J.A.T. Machado, Analysis and design of fractional-order digital control systems, Systems Analysis, Modelling, Simulation 27 (2–3) (1997) 107–122.
[6] R.R. Nigmatullin, The statistics of the fractional moments: is there any chance to read quantitatively any randomness? Signal Processing 86 (10) (2006) 2529–2547.
[7] D. Baleanu, About fractional quantization and fractional variational principles, Communications in Nonlinear Science and Numerical Simulation 14 (6) (2009) 2520–2523.
[8] I. Podlubny, Fractional-order systems and $PI^{\lambda}D^{\mu}$-controllers, IEEE Transactions on Automatic Control 44 (1) (1999) 208–213.
[9] J.A.T. Machado, Discrete-time fractional-order controllers, Fractional Calculus & Applied Analysis 4 (1) (2001) 47–66.
[10] Y.Q. Chen, K.L. Moore, Discretization schemes for fractional-order differentiators and integrators, IEEE Transactions on Circuits and Systems Part I: Fundamental Theory and Applications 49 (3) (2002) 363–367.
[11] C.C. Tseng, Design of fractional order digital FIR differentiators, IEEE Signal Processing Letters 8 (3) (2001) 77–79.
[12] W.S. Torgerson, Theory and Methods of Scaling, Wiley, New York, 1958.
[13] R.N. Shepard, The analysis of proximities: multidimensional scaling with an unknown distance function, Psychometrika 27 (I and II) (1962) 125–140 and 219–246.
[14] J. Kruskal, Multidimensional scaling by optimizing goodness of fit to a nonmetric hypothesis, Psychometrika 29 (1) (1964) 1–27.
[15] J.B. Kruskal, M. Wish, Multidimensional Scaling, Sage Publications, Newbury Park, 1978.
[16] T.F. Cox, M.A.A. Cox, Multidimensional Scaling, Chapman & Hall, CRC, Boca Raton, 2001.
[17] I. Borg, P.J. Groenen, Modern Multidimensional Scaling-Theory and Applications, Springer-Verlag, New York, 2005.
[18] W.L. Martinez, A.R. Martinez, Exploratory Data Analysis with MATLAB, Chapman & Hall, CRC, Boca Raton, 2005.
[19] J. de Leeuw, P. Mair, Multidimensional scaling using majorization: SMACOF in R, Journal of Statistical Software 31 (3) (2009) 1–30.
[20] J.A.T. Machado, A.M.S. Galhano, Approximating fractional derivatives in the perspective of system control, Nonlinear Dynamics 56 (4) (2009) 401–407.
[21] E.D.A.S.H.E.R.G.J. Machado, D. Baleanu, Characterization approach to modified glassy carbon electrode-nanofilm system within multidimensional scaling, Journal of Computational and Theoretical Nanoscience 8 (2) (2011) 1–6.
[22] F.B.D.J.A. Tenreiro Machado, Gonçalo M. Duarte, Identifying economic periods and crisis with the multidimensional scaling, Nonlinear Dynamics 63 (4) (2011) 611–622.
[23] J.M. Smith, Mathematical Modeling and Digital Simulation for Engineers and Scientists, Wiley, New York, 1987.
[24] M.A. Al-Alaoui, Novel digital integrator and differentiator, Electronics Letters 29 (4) (1993) 376–378.
[25] M.A. Al-Alaoui, Filling the gap between the bilinear and the backward-difference transforms: an interactive design approach, International Journal of Electrical Engineering Education 34 (4) (1997) 331–337.
[26] A.M.O.J.K.T.J.A. Tenreiro Machado, Alexandra M. Galhano, Approximating fractional derivatives through the generalized mean, Communications in Nonlinear Science and Numerical Simulations 14 (11) (2009) 3723–3730.
[27] J.A.T. Machado, Visualizing fractional control system approximations by means of multidimensional scaling, in: Proc. of the ASME 2011 International Design Engineering Technical Conferences and Computers and Information in Engineering Conf., Washington, DC, USA, 2011.
[28] S.-H. Cha, Taxonomy of nominal type histogram distance measures, in: Proc. of the American Conference on Applied Mathematics, Harvard, Massachusetts, USA, 2008.